



# Low-density lipoprotein transport within a multi-layered arterial wall—Effect of the atherosclerotic plaque/stenosis



Stephen Chung, Kambiz Vafai\*

Department of Mechanical Engineering, University of California, Riverside, USA

## ARTICLE INFO

### Article history:

Accepted 15 September 2012

### Keywords:

Low-density lipoprotein transport  
Arterial wall  
Atherosclerotic plaque  
Porous media  
Multi-layered model  
Intima fiber matrix

## ABSTRACT

Low-density lipoprotein (LDL) transport while incorporating the thickening of the arterial wall and cholesterol lipid accumulation is analyzed. A multi-layered model is adopted to represent the heterogeneity using the Darcy–Brinkman and Staverman filtration equations to describe transport within the porous layers of the wall. The fiber matrix model is utilized to represent the cholesterol lipid accumulation and the resulting variable properties. The impact of atherosclerotic wall thickening is shown to be negligible in the axial direction, but is found to be considerable in the radial direction within intima. The reference values of intima's porosity and effective fiber radius are obtained through the fiber matrix model, which characterizes the microstructure within the intima. Transport through dysfunctional endothelium and fibrous cap, and the impact on hydraulic and molecular transport properties by LDL accumulation in a thickened arterial wall is analyzed. The effect of variable properties on plasma and LDL molecular transport is also discussed.

© 2012 Elsevier Ltd. All rights reserved.

## 1. Introduction

Cardiovascular disease is a critical issue with respect to human health due to the high rate of death that it causes. Almost 80 million adults in America have one or two types of cardiovascular diseases (American Heart Association, 2007; Khakpour and Vafai, 2008). Atherosclerosis, is a type of cardiovascular disease that usually occurs in a larger artery like aorta and leads to other types of cardiovascular diseases. This aortic disease itself is the 14th cause of death in America (Gillum, 1995; Khanafer et al. 2009), with the subsequent mortality rate increasing by 1–2% per hour after it is discovered (Wang and Dake, 2006; Khanafer and Berguer 2009). Almost half a trillion dollars were spent on health care associated with the cardiovascular diseases in 2008 in the United States (American Heart Association, 2008; Hossain et al., 2011). Clearly, this figure is higher today.

Although the main cause of atherosclerosis is still not fully established, low-density lipoprotein (LDL) is considered to be one of the main factors in causing atherosclerosis. LDL oxidized with free radicals inside the arterial wall damages the cells and compromises the immune response resulting in a dysfunction within the arterial wall and plaque formation thus narrowing the available cross section for lumen flow. In most of the cases, the first symptom of atherosclerosis is a heart attack, and half of these

lead to death. On an annual basis, 1.1 million Americans die from atherosclerosis complications, which accounts for 1/5 of deaths in the United States (American Heart Association, 2005, 2006; Hossain et al., 2011). Therefore, better understanding of the formation of atherosclerosis and stenosis can lead to a better diagnosis and treatment of this disease.

Starting with lipid accumulation, atherosclerosis results a lipid filled plaque that can block blood flow through an artery. Three stages can be cited during development of atherosclerosis: (1) cholesterol lipid accumulation inside arterial wall, specially within the intima layer; (2) thickening of the wall due to component deposits that cause stenosis; and (3) dysfunction of endothelium and fibrous cap formed on the inner wall surface within endothelium and intima (Hossain et al., 2011). Likewise, stenosis can be classified into three grades (Buchanan and Kleinstreuer, 1997): (1) no Stenosis; (2) moderate stenosis; severe stenosis (Ai and Vafai, 2006). Ai and Vafai (2006) had discussed the LDL transport and its deposition within the arterial wall along with variations in its thickness due to plaque formation.

A comprehensive model of LDL accumulation within the arterial wall is crucial in better understanding of the involved processes leading to atherosclerosis. The arterial wall is actually composed of glycocalyx, endothelium, intima, internal elastic lamina (IEL), media, and adventitia, with different hydraulic and mass transport properties. Transport within these layers have been investigated, both from macro-scale view point (Huang et al., 1994; Tada and Tarbell, 2004; Prosi et al., 2005; Ai and Vafai, 2006) as well as a micro-scale point of view (Curry, 1984a, b;

\* Corresponding author. Tel.: +1 951 827 2135; fax: +1 957 827 2899.  
E-mail address: vafai@engr.ucr.edu (K. Vafai).

**Nomenclature**

$c$	LDL concentration
$D$	LDL diffusivity
$G$	Kozney constant
$H$	thickness of the layers
$k$	reaction coefficient
$K$	hydraulic permeability
$L$	length of the artery
$p$	hydraulic pressure
$r$	radial location from the centerline
$r_m$	molecular radius
$r_{CF}$	radius of central filament
$r_{CP}$	radius of proteoglycan core protein
$r_f$	effective intima fiber radius
$r_G$	radius of glycosaminoglycan
$r_M$	effective monomer radius
$R_0$	radius of lumen domain
$u$	axial velocity
$\vec{u}$	velocity vector
$U_0$	maximum velocity at entrance
$v$	filtration (radial) velocity
$x$	axial location from inlet

$x_0$	half width of atherosclerotic plaque
$x_{st}$	axial location of atherosclerotic plaque / stenosis
$\alpha$	length ratio of proteoglycan monomers to central filament
$\beta$	length ratio of glycosaminoglycan fiber to protein core
$\delta$	ratio of maximum thickness of plaque to radius of lumen
$\varepsilon$	porosity
$\phi$	partition coefficient
$\mu$	viscosity
$\sigma$	reflection coefficient
$\Delta$	distance between protein fibers

**Subscripts**

0	refers to entrance condition
<i>eff</i>	refers to effective property
<i>f</i>	refers to plasma property
<i>PG</i>	refers to proteoglycan
<i>CG</i>	refers to collagen
<i>Lip</i>	refers to property affected by LDL lipid accumulation

Fry, 1985; Wen et al., 1988; Huang et al., 1992; Hunag et al., 1997; Huang and Tarbell, 1997; Yuan et al., 1991; Weinbaum et al., 1992; Karner et al., 2001; Liu et al., 2011; Chung and Vafai, 2012). For example, Ai and Vafai (2006) utilized a reverse procedure to solve for hydraulic permeability, effective diffusivity, and reflection coefficient of arterial porous layers using a circuit analogy. On the other hand, Huang et al. (1994), Karner et al. (2001), Liu et al. (2011) and Chung and Vafai (2012) obtained the properties based on the microstructure information using the pore theorem and fiber matrix model.

A number of works (Huang et al., 1994; Karner et al., 2001; Liu et al., 2011) indicate that the arterial transport properties are controlled by the microstructure in each of the different layers of the arterial wall. Several theorems were introduced to enable calculation of the properties based on the parameters that describe the microstructure, such as fiber matrix model for obtaining the properties within the intima layer. However, these focus on transport inside a normal healthy artery only, instead of that under initiation or development of atherosclerosis. The present work invokes the fiber matrix model to obtain intima properties, and additionally analyzes the variation of the fiber matrix parameters to represent the impact by fibers/cells hyperplasia and lipid accumulation due to atherosclerosis. Furthermore, the effects due to a leaky junction (Huang et al., 1994; Chung and Vafai, 2012) and fibrous cap (Hossain et al., 2011) are incorporated into our model to represent the dysfunctional endothelium, which is exposed to arterial lumen. Therefore, utilizing a multi-layered structure, the model introduced in this study can more comprehensively demonstrate the formation of atherosclerosis and its effect on transport within an artery.

A multi-layered model (Ai and Vafai, 2006; Yang and Vafai, 2006, 2008) accurately represents the layered structure with different transport behavior within each of the layers. These layers are endothelium, intima, IEL, and media, where the Staverman–Kedem–Katchalsky membrane equation (Kedem and Katchalsky, 1958) is invoked to describe the mass convection inside a low permeability porous medium. The impact of macrostructure such as stenosis (Ai and Vafai, 2006; Khanafer et al., 2009) or bifurcation (Khakpour and Vafai, 2008) has been studied

by several scientists. However, the macrostructure might not play a significant role, and as an example, in Ai and Vafai's (2006) study the effect of stenosis on LDL transport, was not found to be pronounced. On the other hand, due to atherosclerosis, the fibrous cap and lipid core formed by the hyperplasia of arterial cells and fibers and accumulation of cholesterol lipid inside the arterial wall impacts the microstructure, and further affects the transport properties. In this study based on the multi-layered model, the impact due to changes in the microstructure which results in a variation of transport properties is analyzed comprehensively while studying the effect of atherosclerosis on arterial transport.

In summary, the current work aims at analyzing the impact of atherosclerotic plaque on LDL transport. The present work, in addition to considering the macrostructure effect, which has been partially discussed before, looks into the microstructure variation due to molecular accumulation and its effect on LDL transport. The impact of stenosis formation, thickening of intima, and transport properties variations due to LDL accumulation associated with atherosclerosis, as well as consideration of the dysfunctional endothelium and fibrous cap, is investigated through an advanced model.

**2. Formulation****2.1. Multi-layer model**

The layered structure of the wall for an artery is shown in Fig. 1, from inner to the outer side, we have lumen, glycocalyx, endothelium, intima, IEL, media, and adventitia. In the present work, glycocalyx is neglected due to its negligible thickness (Michel and Curry, 1999; Tarbell, 2003), and adventitia is embedded into the boundary condition on the outer surface of the wall due to its low resistance (Yang and Vafai, 2006, 2008; Ai and Vafai, 2006). The lumen domain is considered as a cylindrical geometry with radius of  $R_0$  (310  $\mu\text{m}$ ) and axial length  $L$  (0.2232 m), surrounded by the porous layers of endothelium, intima, IEL, and media with their detailed information given in Table 1a (Karner et al., 2001; Prosi et al., 2005; Yang and Vafai, 2006,

2008; Ai and Vafai, 2006; Chung and Vafai, 2012). It should be noted that intima properties given in this table are only used for validation with previous works, as it will be based on fiber matrix theory for later results.

## 2.2. Atherosclerotic plaque and stenosis

To study LDL transport inside a diseased artery, a computational domain similar to that used in Ai and Vafai's (2006) work is utilized as shown in Fig. 2a. The atherosclerotic plaque is considered by a partial wall thickening within the intima layer that causes stenosis, characterized by  $\delta$ , ratio of maximum thickness to lumen radius,  $x_{st}$ , its axial location from inlet, and  $x_0$ , its half width. However, Ai and Vafai (2006) considered the transport properties of all arterial layers within a normal artery when cholesterol lipid accumulation is not considered. In this

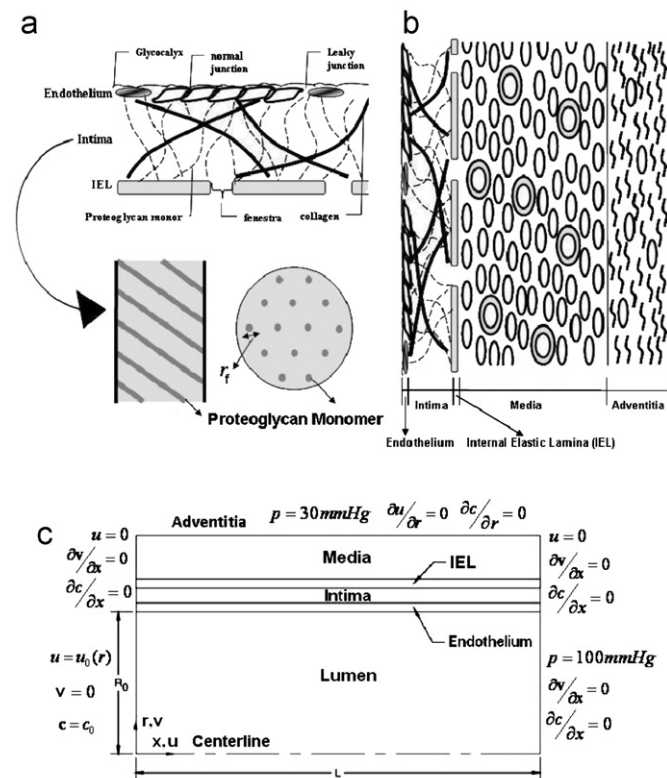


**Fig. 1.** Configuration for (a) Endothelium, intima, IEL, and intima fiber matrix; (b) Arterial wall; (Chung and Vafai, 2012); (c) Analyzed domain for a healthy artery (Yang and Vafai, 2006; Ai and Vafai, 2006).

**Table 1**

(a) Hydraulic and LDL transport properties for each of the layers/domains (Ai and Vafai, 2006; Chung and Vafai, 2012); (b) Properties obtained in previous works for dysfunctional endothelium and fibrous cap.

(a)	Lumen	Endothelium	Intima	IEL	Media
Diffusivity $D_{eff}$ ( $m^2/s$ )	$2.87 \times 10^{-11}$	$8.154 \times 10^{-17}$	$5 \times 10^{-12}$	$3.18 \times 10^{-15}$	$5 \times 10^{-14}$
Permeability $K$ ( $m^2$ )		$3.2172 \times 10^{-21}$	$2.2 \times 10^{-16}$	$3.2188 \times 10^{-19}$	$2 \times 10^{-18}$
Reflection coefficient $\sigma$		0.9886	0.8292	0.8295	0.8660
Thickness $H$ ( $\mu m$ )	3100	2	10	2	200
Viscosity $\mu_{eff}$ ( $kg/m \cdot s$ )	$3.5 \times 10^{-3}$	$0.72 \times 10^{-3}$	$0.72 \times 10^{-3}$	$0.72 \times 10^{-3}$	$0.72 \times 10^{-3}$
(b)	<b>Normal endothelium</b>	<b>Leaky endothelium</b>	<b>Fibrous cap</b>		
Thickness ( $\mu m$ )	2		65		
Hydraulic permeability ( $m^2$ )	$3.21 \times 10^{-21}$	$2.62 \times 10^{-19}$	–		
Effective diffusivity ( $m^2/s$ )	$8.15 \times 10^{-17}$	$1.142 \times 10^{-14}$	$4.5 \times 10^{-13}$		
Reflection coefficient	0.9886	0.7240	–		
References	Ai and Vafai (2006)	Curry (1984a, b), Chung and Vafai (2012)	Hossain et al. (2011)		

work, the lipid filling effect is brought in by applying the fiber matrix theory within a computational domain that incorporates the multi-layered structure of the diseased arterial wall as shown in Fig. 2d.

## 2.3. Governing equations

A steady state assumption is invoked based on the negligible effect of blood pulsation (Yang and Vafai, 2006; Chung and Vafai, 2012). The hydraulic and molecular transport in the lumen region is described by conservation of mass, momentum and species as

$$\begin{aligned} \nabla \cdot \vec{u} &= 0 \\ -\nabla p + \mu_f \nabla^2 \vec{u} &= 0 \\ \vec{u} \cdot \nabla c &= D_f \nabla^2 c \end{aligned} \quad (1)$$

where  $\vec{u}$  is the velocity vector,  $c$  is the LDL concentration,  $p$  is the hydraulic pressure, and  $\mu_f$  and  $D_f$  are the plasma viscosity and diffusivity coefficient, respectively.

The flow and mass transfer governing equations within the four layers, endothelium, intima, IEL, and media, can be represented by Darcy–Brinkman equation while incorporating the Staverman–Kedem–Katchalsky membrane equation (Kedem and Katchalsky, 1958):

$$\begin{aligned} \nabla \cdot \vec{u} &= 0 \\ -\nabla p + \mu_{eff} \nabla^2 \vec{u} - \frac{\mu_{eff}}{K} \vec{u} &= 0 \\ (1-\sigma) \vec{u} \cdot \nabla c &= D_{eff} \nabla^2 c - kc \end{aligned} \quad (2)$$

where  $\mu_{eff}$  is the effective fluid viscosity,  $K$  hydraulic is the permeability;  $\sigma$  is the reflection coefficient;  $D_{eff}$  is the effective LDL diffusivity,  $k$  is the reaction coefficient which is  $3.197 \times 10^{-4}$  ( $s^{-1}$ ) inside the media layer and zero in the other layers (Prosi et al., 2005; Yang and Vafai, 2006, 2008). The property values for each of the layers are listed in Table 1a, while the variable intima properties due to the lipid accumulation are considered later in this work. The flow and molecular transport characteristics within the layers under the influence of lipid accumulation such as the fibrous cap are also described by Eq. (2) and the corresponding properties are given in Table 1b.

## 2.4. Boundary conditions

The boundary conditions are illustrated in Fig. 1, where the axial velocity  $u$  at the entrance is considered to have a fully developed profile  $u_0(r)$  expressed by

$$u_0 = U_0 \left( 1 - (r/R_0)^2 \right) \text{ at } x=0, 0 \leq r \leq R_0 \quad (3)$$

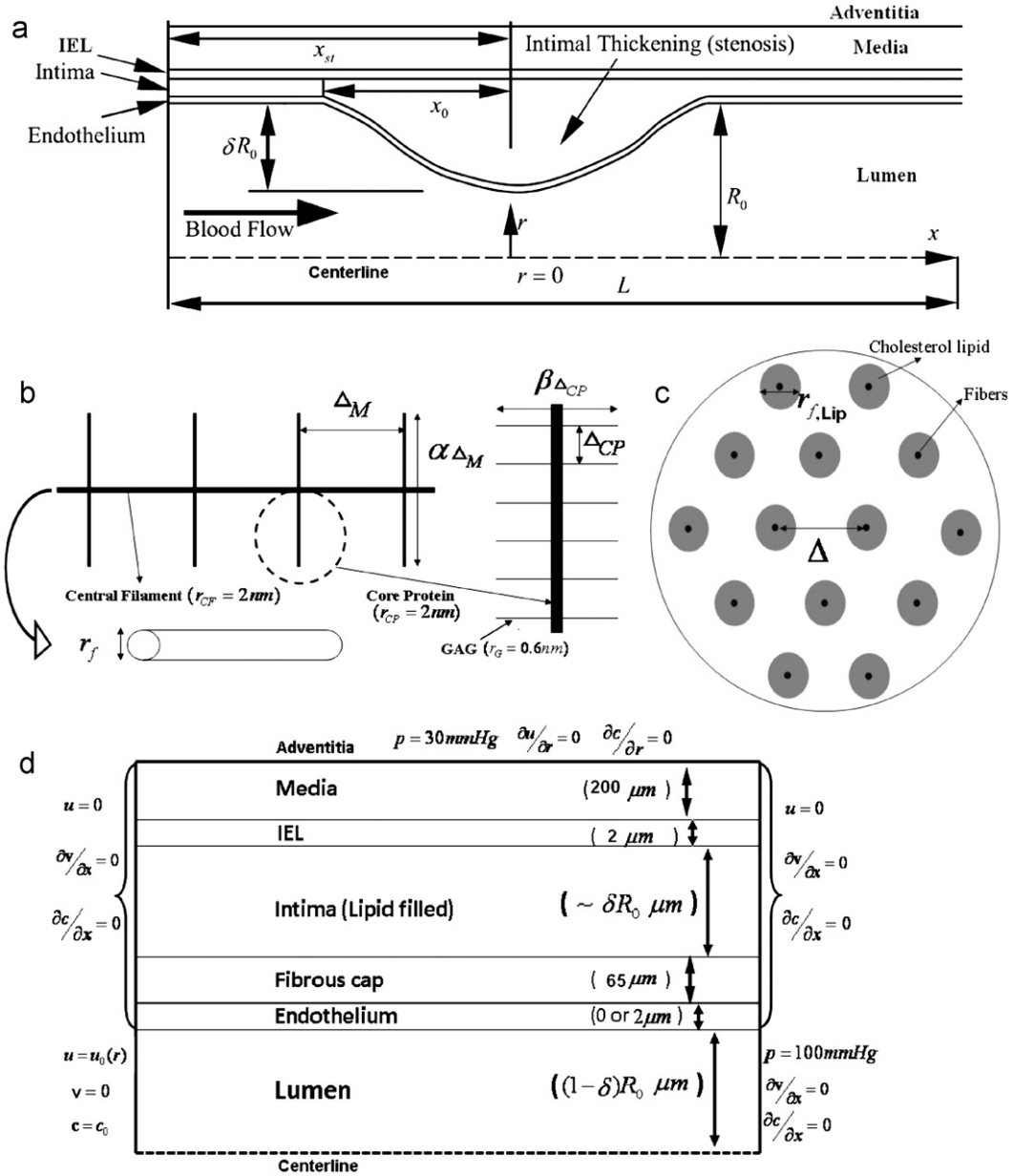


**Fig. 2.** Configuration for (a) Analyzed domain in the presence of stenosis (Ai and Vafai, 2006); (b) Proteoglycan fibers within intima (Huang et al., 1994); (c) Fiber matrix filled with cholesterol lipid; (d) Analyzed region for the stenosis/plaque case.

where the maximum entrance velocity  $U_0$  is taken as 0.338 m/s (Yang and Vafai, 2006; Karner et al., 2001) and LDL concentration at the entrance  $c_0$  is taken as  $28.6 \times 10^{-3} \text{ mol/m}^3$  (Katz, 1985; Tarbell, 1993; Yang and Vafai, 2006). Hydraulic pressure  $p$  is set to be fixed at the outlet of lumen and the outer surface (media-adventitia interface) with the values of 100 mm Hg and 30 mm Hg resulting in a total pressure drop of 70 mm Hg through the arterial wall (Meyer et al., 1996; Yang and Vafai, 2006). Continuity conditions for the flow and mass transfer are invoked at the interface between each of the layers while incorporating the Staverman filtration condition (Yang and Vafai, 2006; Chung and Vafai, 2012) as

$$\left[ (1-\sigma)vc - D_{eff} \frac{\partial c}{\partial r} \right]_+ = \left[ (1-\sigma)vc - D_{eff} \frac{\partial c}{\partial r} \right]_- \quad (4)$$

where  $v$  is the filtration velocity of the blood flow penetrating through the arterial wall in the radial direction.

### 2.5. Fiber matrix model and intima properties

The intima is mainly formed by proteoglycan fibers (Fig. 2), and looser-thicker collagen fibers (Frank and Fogelman, 1989), which can be represented as a homogeneous fiber matrix as shown in Fig. 1a. Compared to endothelium and IEL, Ai and Vafai (2006) pointed out that diffusion in intima layer is not substantial, which was also confirmed in Yang and Vafai's (2006) study. The microstructure of intima fiber matrix can be characterized by its porosity  $\varepsilon$  and effective fiber radius  $r_f$ . A common way to calculate the effective radius of intima protein,  $r_f$  (Huang et al., 1994; Dabagh et al., 2009) is

$$r_f = \left[ \frac{\alpha r_M^2 + r_{CF}^2}{\alpha + 1} \right]^{1/2} \quad (5a)$$

where  $\alpha$  is the length ratio of proteoglycan monomers to central filament, with a value which is variant between 3 and 10

(Lark et al., 1988),  $r_{CF}$  is radius of central filament with a value around 2 nm (Buckwalter and Rosenberg, 1982), and  $r_M$  is the effective monomer radius calculated by

$$r_M = [\beta r_G^2 + r_{CP}^2]^{1/2} \tag{5b}$$

where  $\beta$  is the length ratio of glycosaminoglycan (GAG) fiber to protein core with a value which is variant between 5 and 10 (Lark et al., 1988),  $r_G$  is radius of GAG with a value of 0.6 nm,  $r_{CP}$  is radius of proteoglycan core protein with a value of 2 nm (Buckwalter and Rosenberg, 1982). By taking  $\alpha=3$  and  $\beta=5$  (Dabagh et al., 2009; Liu et al., 2011), we can obtain the effective fiber radius for proteoglycan as 2.31 nm.

Utilizing the Carman–Kozney equation (Curry and Michel, 1980; Curry, 1984a, b), the intima’s permeability can be calculated as

$$K = \frac{r_f^2 \varepsilon^3}{4G(1-\varepsilon)^2} \tag{6a}$$

where  $\varepsilon$  is the porosity of intima, and  $G$  is the Kozney constant which, for randomly oriented fibers, is calculated as (Happel and Brenner, 1965)

$$G = \frac{2}{3} \frac{2\varepsilon^3}{(1-\varepsilon)[2\ln(1/1-\varepsilon)-3+4(1-\varepsilon)-(1-\varepsilon)^2]} + \frac{1}{3} \frac{2\varepsilon^3}{(1-\varepsilon)[\ln(1/1-\varepsilon)-(1-(1-\varepsilon)^2)/(1+(1-\varepsilon)^2)]} \tag{6b}$$

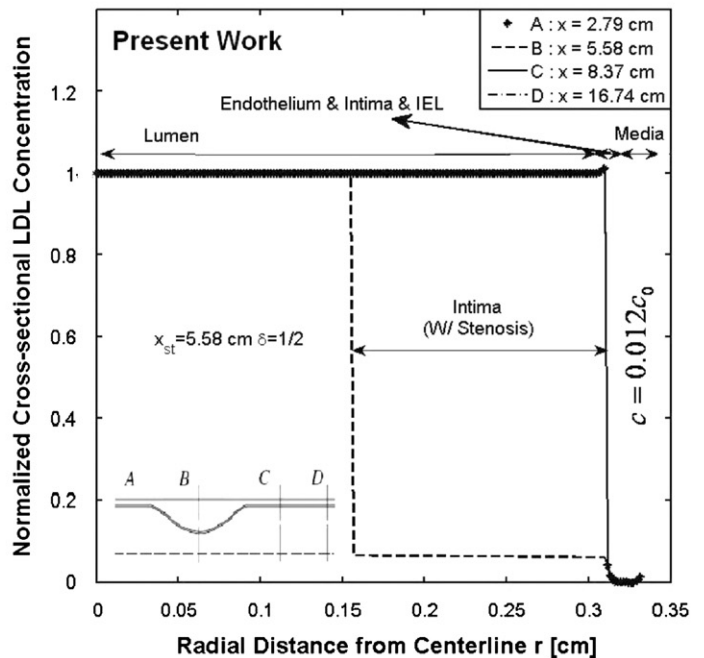
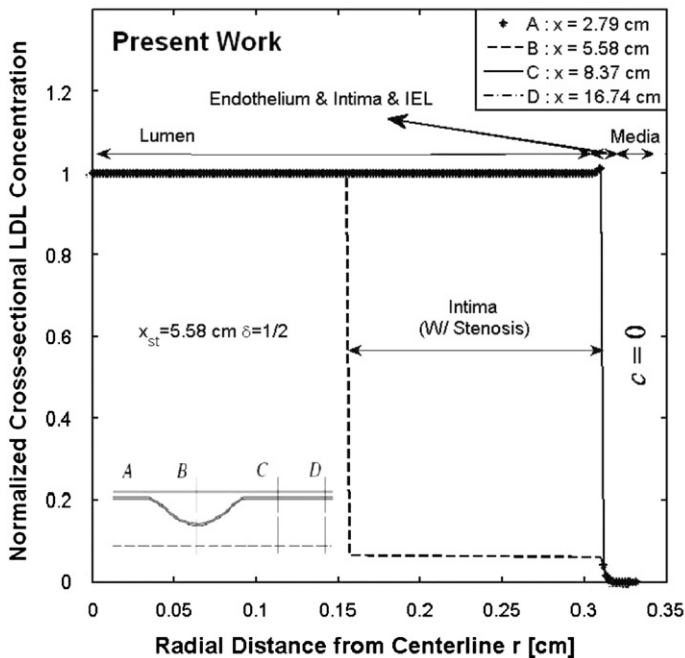
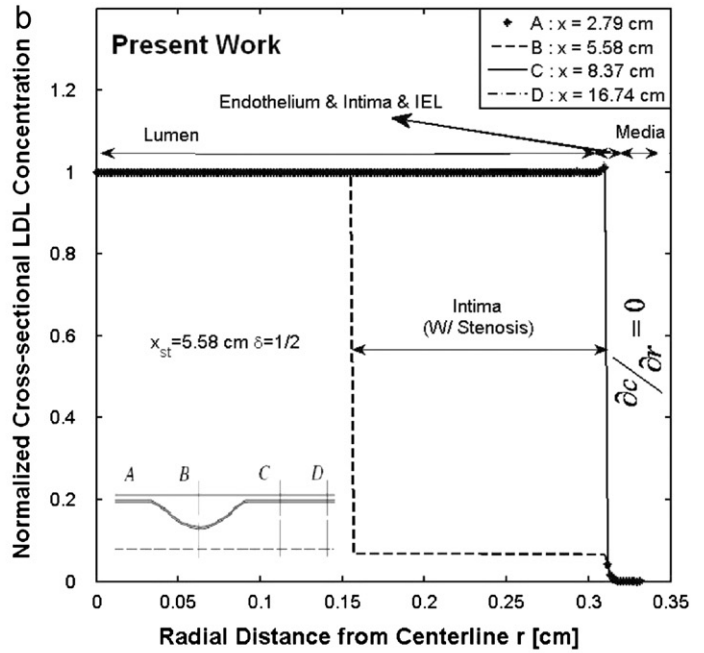
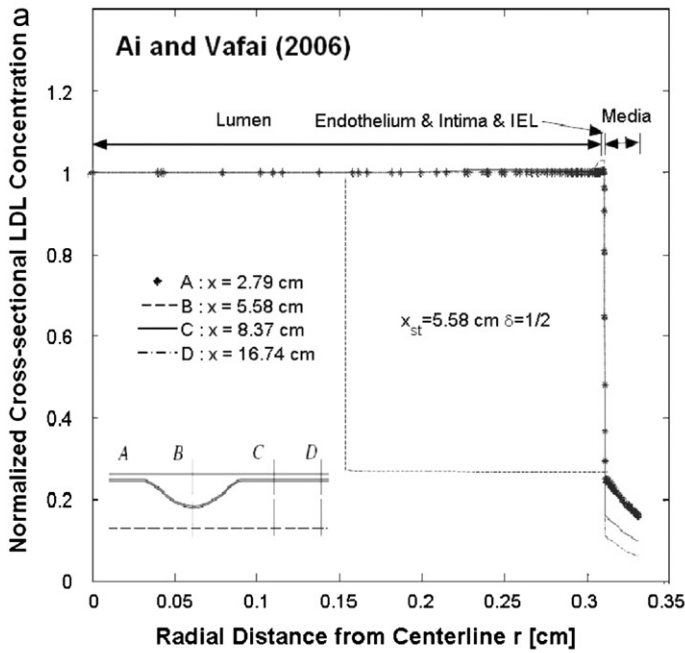


Fig. 3. Normalized LDL concentration  $c/c_0$  across diseased artery layers in the presence of stenosis with  $\delta=0.5$ ,  $x_{st}=5.58$  cm and  $x_0=2R_0$ : (a) for comparison with Ai and Vafai (2006) work; (b) for two different boundary conditions at the media–adventitia interface ( $r=3.314$  mm)  $c=0$  &  $c=0.012c_0$ .

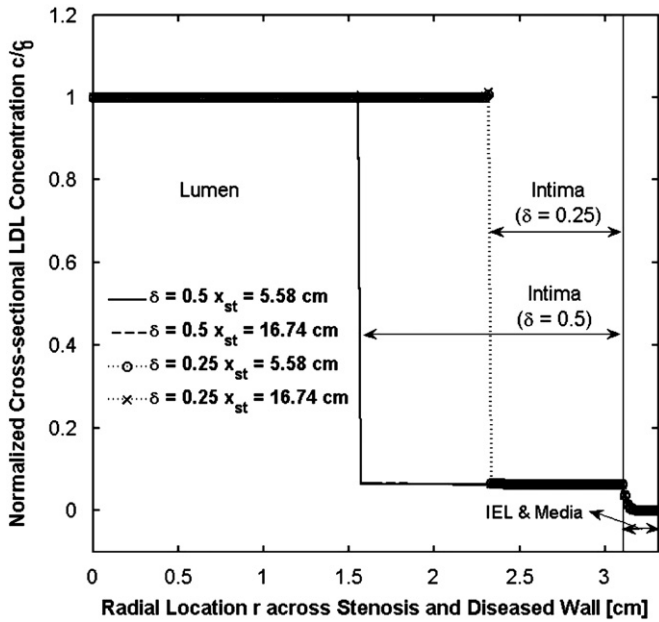


Fig. 4. Normalized LDL concentration  $c/c_0$  across diseased artery layers in the presence of stenosis at center of the plaque ( $x = x_{st}$ ;  $x_0 = 2R_0$ ) with different wall thickening  $\delta$  and location of stenosis  $x_{st}$ .

The molecular transport properties for LDL particle through intima, such as the effective diffusivity  $D_{eff}$  and reflection coefficient  $\sigma$  can be calculated by (Huang et al., 1992, 1994)

$$D_{eff} = D_f \exp \left[ -(1-\varepsilon)^{1/2} \left( 1 + \frac{r_m}{r_f} \right) \right] \quad (7a)$$

$$\sigma = (1-\phi)^2 \quad (7b)$$

where  $r_m$  is LDL molecular radius taken as 11 nm (Huang et al., 1992, 1994), and  $\phi$  is the partition coefficient obtained by

$$\phi = \exp \left[ -(1-\varepsilon) \left( \frac{2r_m}{r_f} + \frac{r_m^2}{r_f^2} \right) \right] \quad (7c)$$

In the work of Dabagh et al. (2009) and Liu et al. (2011), in addition to proteoglycan fibers, the collagen fibers are also considered. As such the transport properties were calculated as

$$\frac{1}{K} = \frac{1}{K_{PG}} + \frac{1}{K_{CG}} \quad (8a)$$

$$D_{eff} = D_f \exp \left[ -(1-\varepsilon_{PG})^{1/2} \left( 1 + \frac{r_m}{r_f} \right) \right] (\varepsilon_{PG} + \varepsilon_{CG} - 1) \exp \left[ -(1-\varepsilon_{CG})^{0.5} \left( 1 + \frac{r_m}{r_{CG}} \right) \right] \quad (8b)$$

$$\sigma = (1-\phi)^2 \quad (8c)$$

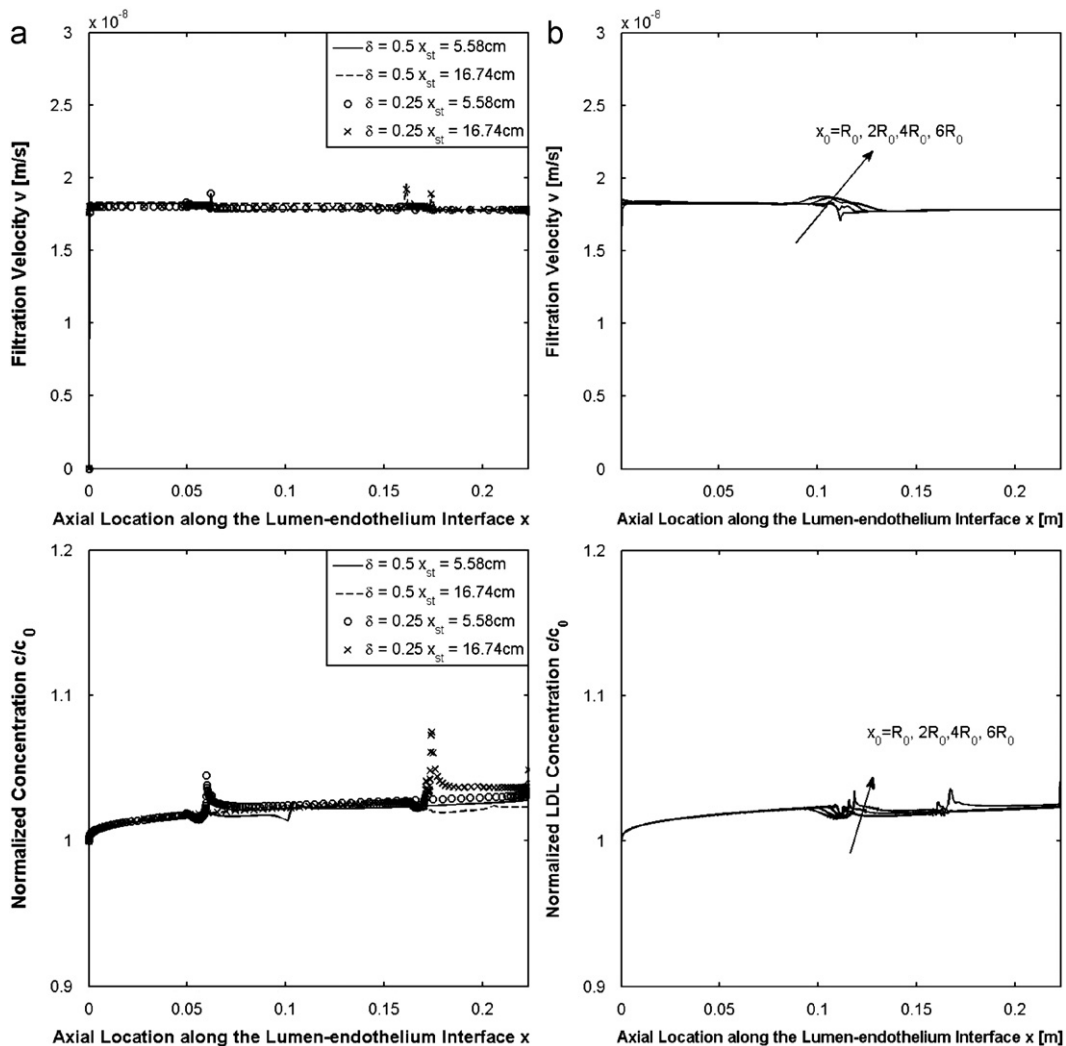


Fig. 5. Filtration velocity, and LDL concentration along the lumen–endothelium interface for (a) different wall thickening ratio  $\delta$  and stenosis locations  $x_{st}$  and (b) different values of the plaque half widths  $x_0$ .

$$\phi = \exp \left[ -(1 - \varepsilon_{PG}) \left( \frac{2r_m}{r_f} + \frac{r_m^2}{r_f^2} \right) (\varepsilon_{PG} + \varepsilon_{CG} - 1) \right] \times \exp \left[ -(1 - \varepsilon_{CG})^{0.5} \left( 1 + \frac{r_m}{r_{CG}} \right) \right] \quad (8d)$$

where  $\varepsilon_{PG}$  and  $\varepsilon_{CG}$  are the porosity of proteoglycan and collagen fibers, and  $r_{CG}$  is radius of collagen fiber set as 20 nm (Dabagh et al., 2009). Also,  $K_{PG}$  and  $K_{CG}$  are calculated through Eqs. (6a and b), using  $\varepsilon_{PG}$  and  $\varepsilon_{CG}$  as the porosity and  $r_f$  and  $r_{CG}$  as the fiber radius. However, due to a much coarser distribution of collagen fibers, it is considered to have an insignificant impact. Therefore, an alternative way is to use Eqs. (6a and b) and (7a–c) with porosity defined by  $\varepsilon = \varepsilon_{PG}\varepsilon_{CG}$  (Dabagh et al., 2009).

### 3. Comparisons

The results for the velocity field and mass concentration are obtained numerically with relative and absolute errors less than  $10^{-3}$  and  $10^{-6}$ , respectively. The model developed in this work is compared with the work of Ai and Vafai (2006) for both normal artery [presented in Chung and Vafai (2012)] and diseased artery with stenosis, using a different solution methodology. The results from both of the cited works show an insignificant impact as a result of either thickening of the wall or different stenosis

locations (Fig. 3a), even with different boundary conditions on the outer surface (adventitia side,  $r = 3.314$  mm) that is commonly applied (Fig. 3b). The methodology utilized in the current study in analyzing LDL transport inside an artery was validated in the work of Chung and Vafai (2012).

## 4. Results and discussion

### 4.1. Sensitivity study on plaque geometry and model simplification

Various researchers have modeled the artery both with and without atherosclerosis; however, mostly modeling it as a wall-free or simplified-wall model, which does not allow them to look into the highly pertinent transport behavior within the arterial wall. In Fig. 4, the impact of the macrostructure, i.e., the shape of stenosis due to atherosclerosis, is shown to be negligible. Fig. 5, which zooms into the lumen–wall interface for pressure, filtration velocity, and LDL concentration, still shows that this effect is negligible.

On the other hand, the impact of the atherosclerosis is shown to be present within the intima as shown in Fig. 6 due to a smaller exposed surface area of the wall to lumen caused by the radial wall thickening. Along the intima–IEL interface, the pressure, filtration velocity and LDL concentration display a significant

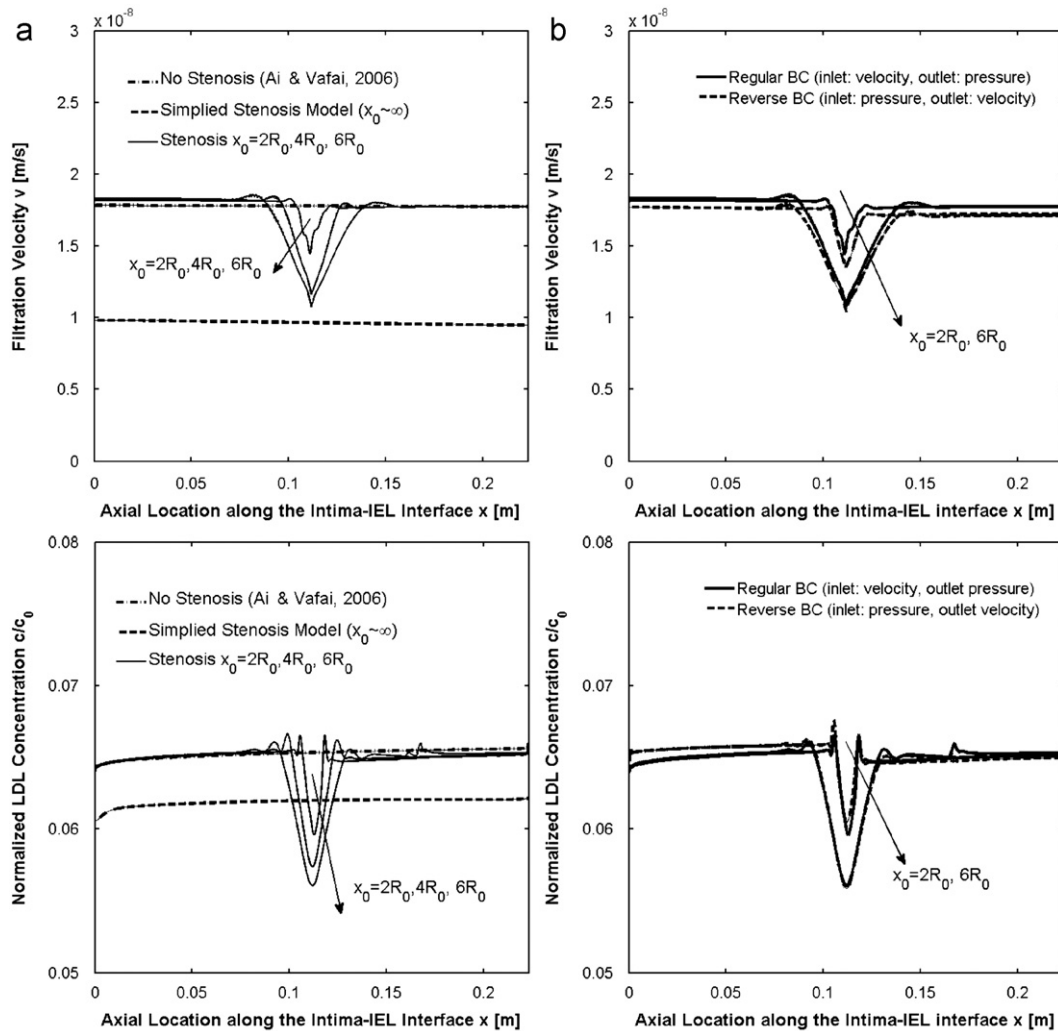


Fig. 6. Filtration velocity and LDL concentration profile along the intima–IEL interface with (a) different plaque half widths  $x_0$  and (b) reversed boundary conditions (inlet: pressure, outlet: velocity).

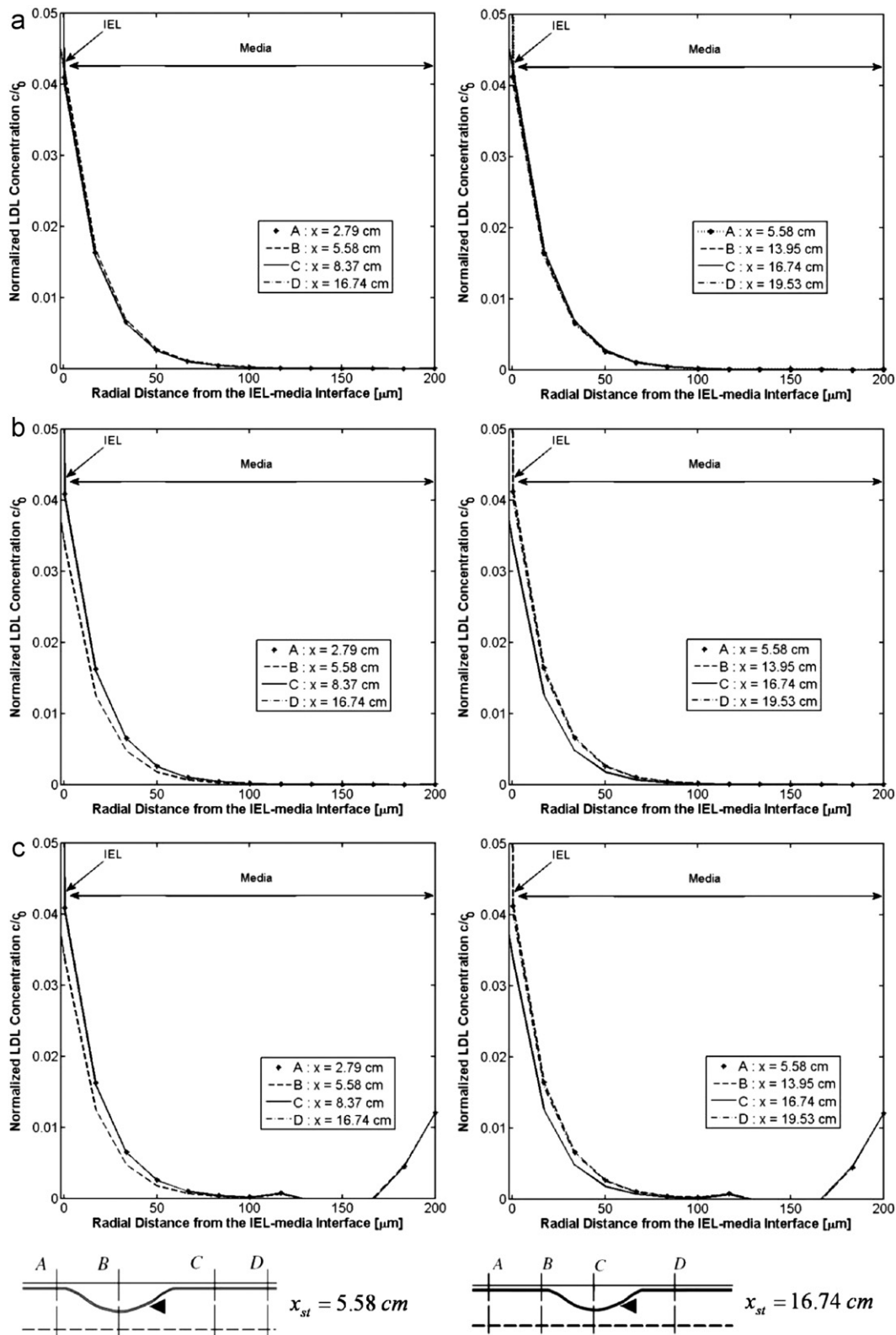


Fig. 7. Normalized LDL concentration  $c/c_0$  across IEL and media of a diseased artery at different locations  $x$  in the presence of stenosis with  $\delta=0.5$ ,  $x_{st}=5.58$  cm and  $16.74$  cm for three different boundary conditions at the media–adventitia interface ( $r=3.314$  mm) as  $\partial c/\partial r=0$ ,  $c=0$ ,  $c=0.012c_0$ .

drop as seen in Fig. 6a. Furthermore, this drop becomes more pronounced as the plaque builds up. Fig. 6b shows that using the reverse boundary conditions at the inlet (specifying pressure instead of velocity) and outlet (specifying velocity instead of pressure), displays the same phenomena seen in Fig. 6a, and

confirms the fact that the edge effects are insignificant. However, this impact diminishes further inside the IEL and intima layers shown in Fig. 7, which shows the effect of boundary condition is also negligible. Therefore, one can conclude that the axial location has a negligible effect on the results.

In conclusion, the atherosclerotic impact at the lumen–wall interface is shown to be minor, compared to the concentration distribution within each different layer of the wall. The present results show that the thickening of the arterial wall impacts plasma and LDL transport in the radial direction substantially more than in the axial direction. As such, a simplified computational domain shown in Fig. 2d can be applied. On the other hand, the microstructure and the transport properties of the arterial layers are impacted by atherosclerosis either by cholesterol lipid accumulation and tissue hyperplasia, or the dysfunction of endothelial layer, which is discussed in detail in the present work.

#### 4.2. Dysfunctional endothelium and fibrous cap

Dysfunctional endothelium and fibrous cap forms as LDL cholesterol deposits accumulate within intima (Hossain et al., 2011). The transport properties of normal junction (Ai and Vafai, 2006) and leaky junction endothelium (Curry, 1984a; Chung and Vafai, 2012), as well as effective diffusivity of fibrous cap (Hossain et al., 2011) are listed in Table 1b. Fig. 8 shows comparison between results obtained for dysfunctional endothelium and fibrous cap on penetration of blood and LDL. The comparison shows that dysfunctional endothelium causes a deduction of the resistance from lumen into wall, while fibrous cap results an increasing resistance.

#### 4.3. Calculation of intima properties through fiber matrix model

Using healthy intima (no cholesterol/lipid accumulation) microstructure characteristics, effective fiber radius  $r_f$  and porosity  $\varepsilon$  are used as a reference point, the transport property values are obtained based on the microstructure information through the fiber matrix method. Table 2a lists intima properties obtained from Eqs. (6a and b) and (7a–c) (considering only the proteoglycan fiber), or Eqs. (8a–d) (considering both proteoglycan and collagen fibers) with effective fiber radius  $r_f$  obtained from Eqs. (5a and b) as 2.31 nm, and the porosity taken from the following prior works: (1)  $\varepsilon=0.983$  (Karner et al., 2001; Yang and Vafai, 2006); (2)  $\varepsilon_{PG}=0.9568$  and  $\varepsilon_{CG}=0.8387$  (Dabagh et al., 2009; Liu et al., 2011); (3)  $\varepsilon_{PG}=0.9866$  and  $\varepsilon_{CG}=0.95$  (Dabagh et al., 2009); (4)  $\varepsilon=\varepsilon_{PG}\varepsilon_{CG}=0.9373$  (Dabagh et al., 2009).

Fig. 9a illustrates the filtration velocity and LDL concentration along the endothelium–intima interface utilizing the data given in Table 2a, compared with the works of Ai and Vafai (2006) and Liu et al. (2011) given in Table 2c. As can be seen in Fig. 9a, even though the intima property values are quite different, as seen in Table 2, the impact on plasma and LDL molecular transport is limited.

Ai and Vafai (2006) pointed out that, within the intima layer, the transport is mostly dominated by convection flux, and their analytical work resulted in a reflection coefficient  $\sigma$  of 0.8292. As such, from the results given in Table 2a, case 2 ( $\varepsilon=\varepsilon_{PG}\varepsilon_{CG}=0.8025$ ) and case 4 ( $\varepsilon=0.9397$ ) are selected for comparison with the results of Ai and Vafai (2006). Utilizing Eqs. (7b) and (7c), with the intima reflection coefficient of 0.8292 and porosities  $\varepsilon$  of 0.9373 and 0.8025, results in an effective radius of intima protein fiber  $r_f$  as 2.08 and 4.17 respectively [nm]. These are represented in Table 2b based on Eqs. (6a and b) and (7a–c).

Fig. 9b show the comparisons for both filtration velocity and LDL concentration at the endothelium–intima interface using the data given in Table 2b. A perfect agreement is seen with the results of Ai and Vafai (2006) and Liu et al. (2011). It should be noted that since a fiber radius of 2.08 nm is closer to the value which is obtained through Eqs. (5a and b), which is also utilized in Yang and Vafai's (2006) work, it is more reasonable to assign the

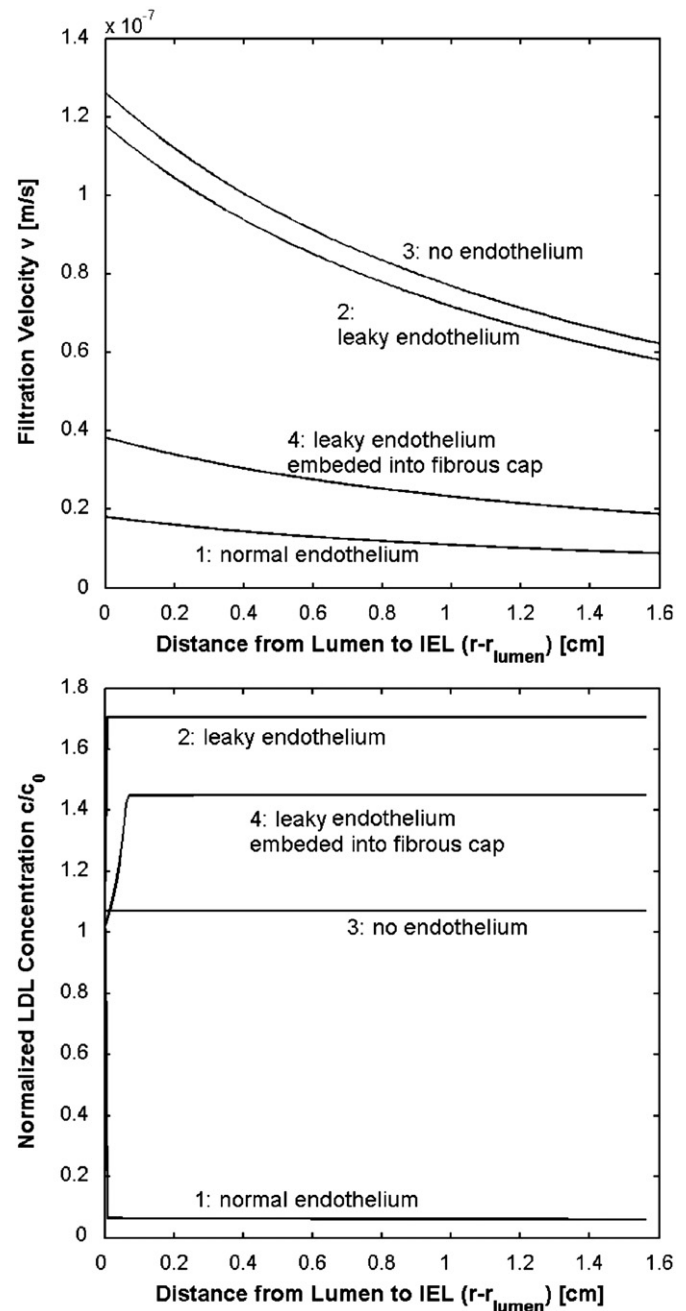


Fig. 8. Filtration velocity and LDL concentration across endothelium, fibrous cap, and intima for different physical attributes of endothelium and fibrous cap given in Table 1b.

porosity  $\varepsilon$  and effective fiber radius  $r_f$  for a healthy intima as 0.9373 and 2.08 nm.

#### 4.4. Impact of variations in intima properties by lipid accumulation

The structure of intima for a normal artery is shown in Fig. 1a, while during LDL molecule accumulation, the structure resembles the schematic shown in Fig. 2c displaying a thicker fiber radius  $r_{f,Lip}$  and a lower porosity  $\varepsilon_{Lip}$  due to the lipid deposits as compared to a healthy intima ( $\varepsilon$  and  $r_f$ ). As discussed earlier, the normal intima porosity  $\varepsilon$  and the effective fiber radius  $r_f$  are set as 0.9397 and 2.08 nm. The maximum fiber thickening ratio ( $r_{f,Lip}/r_f$ ) is set as 150 which is the ratio of the thickness of atherosclerotic

**Table 2**

Intima properties (a) obtained using fiber matrix method with protein fiber radius  $r_f$  of 2.31 nm (Eq. (5a and b)) and variation of intima porosity,  $\varepsilon$  or ( $\varepsilon_{PG}$ ,  $\varepsilon_{CG}$ ) given in previous work (Yang and Vafai, 2006; Dabagh et al., 2009); (b) obtained using fiber matrix method variations in both intima porosity  $\varepsilon$  (Dabagh et al., 2009,  $\varepsilon = \varepsilon_{PG}\varepsilon_{CG}$ ) and protein fiber radius  $r_f$ ; (c) obtained in the prior works (Ai and Vafai, 2006; Liu et al., 2011).

#	Porosity $\varepsilon$ or ( $\varepsilon_{PG}$ , $\varepsilon_{CG}$ )	Effective fiber radius (nm)	Permeability $K$ ( $m^2$ )	Diffusivity $D_{eff}$ ( $m^2/s$ )	Reflection coefficient $\sigma$
(a)					
1	0.983	2.31	$1.66 \times 10^{-16}$	$1.35 \times 10^{-11}$	0.1771
2	(0.9568, 0.8387)	2.31	$3.93 \times 10^{-17}$	$3.7 \times 10^{-12}$	0.7983
3	(0.9866, 0.95)	2.31	$2.1 \times 10^{-16}$	$9.7 \times 10^{-12}$	0.3247
4	0.9373	2.31	$2.5 \times 10^{-17}$	$6.78 \times 10^{-12}$	0.7512
(b)					
1	0.9373	2.08	$2.02 \times 10^{-17}$	$5.94 \times 10^{-12}$	0.8292
2	0.8025	4.17	$9.59 \times 10^{-18}$	$5.7 \times 10^{-12}$	0.8292
(c)					
Ai and Vafai (2006)	0.96	–	$2.2 \times 10^{-16}$	$5 \times 10^{-12}$	0.8292
Liu et al. (2011)	(0.9568, 0.8387)	–	$4.2 \times 10^{-17}$	$3.7 \times 10^{-12}$	0.7983

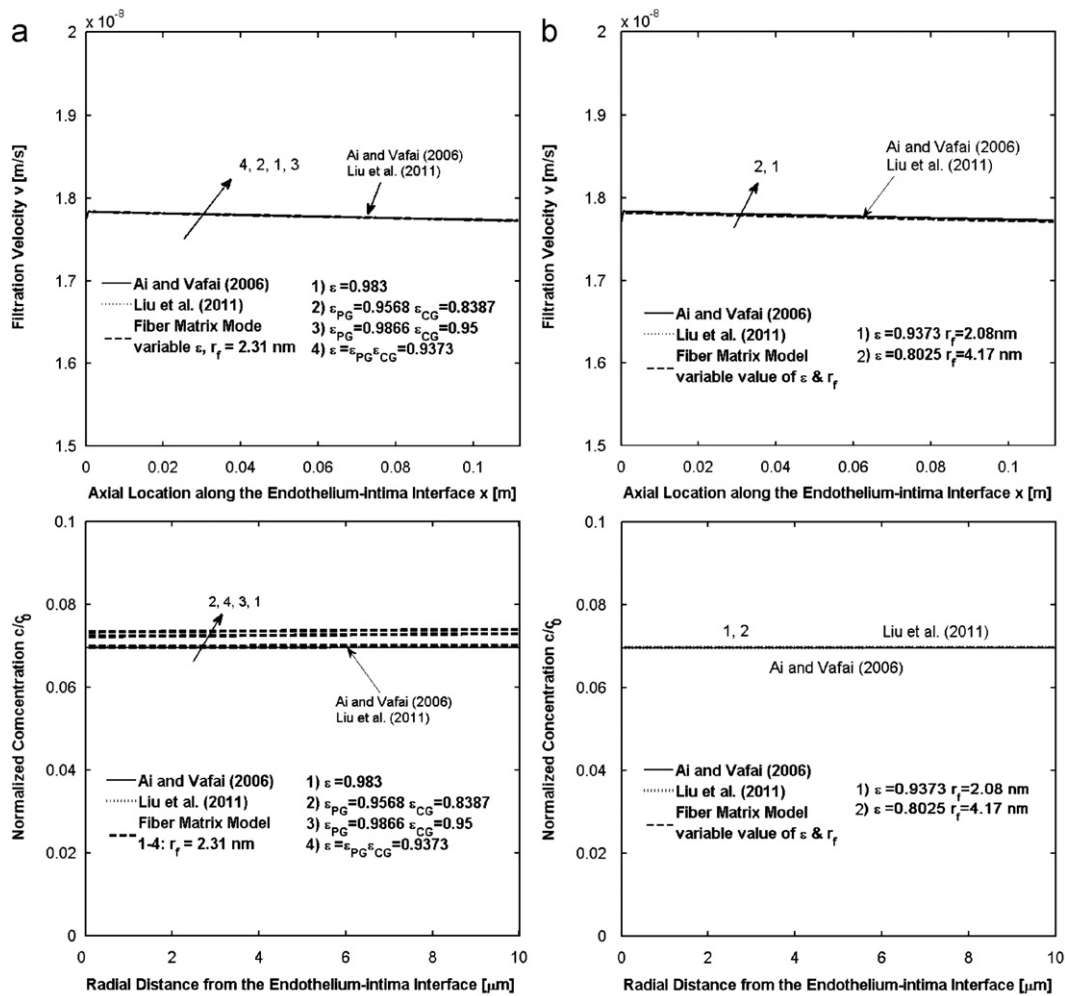


**Fig. 9.** Filtration velocity and LDL concentration along the intima–IEL interface. Intima properties were obtained through fiber matrix model with (a) protein fiber radius  $r_f$  of 2.31 nm and variations of intima porosity,  $\varepsilon$  or ( $\varepsilon_{PG}$ ,  $\varepsilon_{CG}$ ) based on data given in Table 2a and (b) variations of intima porosity  $\varepsilon$  and effective protein fiber radius  $r_f$  based on data given in Table 2b, and compared with those based on the properties obtained by Ai and Vafai (2006) and Liu et al. (2011) given in Table 2c.

plaque with  $\delta=0.5$  to the thickness of a normal intima layer. With the effective intima porosity  $\varepsilon_{Lip}$  and protein fiber thickening rate  $r_{f,Lip}/r_f$  varying between 20–93.97% and 1–150, respectively, the variable properties for the hydraulic permeability  $K$ , effective

diffusivity  $D_{eff}$ , and reflection coefficient  $\sigma$  are obtained through fiber matrix model using Eqs. (6a and b) and (7a–c).

To describe LDL transport within a diseased artery (Fig. 2d), A fibrous cap with an embedded dysfunctional endothelium (model

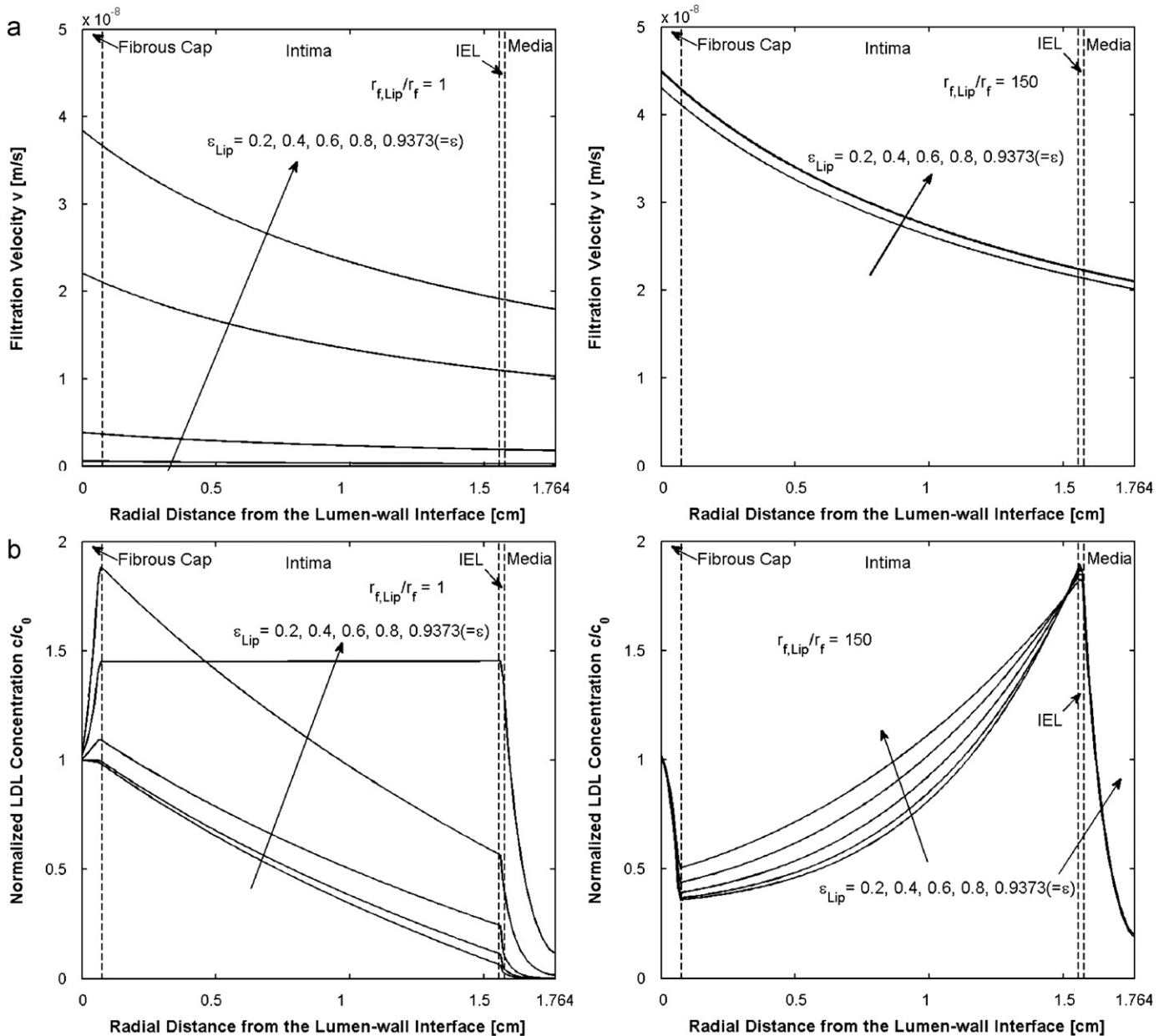


**Fig. 10.** Effect of variations in the effective porosity  $\epsilon_{Lip}$  and protein fiber thickening ratio  $r_{f,Lip}/r_f$  on the (a) filtration velocity and (b) the LDL molecule concentration, across a diseased arterial wall.

4 in Fig. 8) is selected to represent the transport properties. Fig. 10a illustrates the impact of variable properties due to lipid accumulation on filtration velocity subject to different effective intima porosity  $\epsilon_{Lip}$  and protein fiber thickening ratio  $r_{f,Lip}/r_f$ . As can be seen in Fig. 10a, a lower porosity leads to a lower permeability, while a thicker effective fiber radius reduces this impact by providing a larger space between the fibers.

Fig. 10b displays the effect of variable properties on the LDL transport. As expected, a higher porosity results in more LDL molecule deposits inside the arterial wall. As the thickening ratio  $r_{f,Lip}/r_f$  increases, a larger space between the fibers is created resulting in a reduction in the selective behavior for LDL particles inside the intima due to formation of stenosis. As such, LDL particles are deposited more near the intima–IEL interface, instead of the inner wall surface, because the IEL layer with its higher rate of the particle selection takes over the role of blocking LDL particle migration from the lumen side.

## 5. Conclusions

Our model clearly demonstrates in detail how cholesterol lipid caused by molecular accumulation affects the microstructure, as well as the LDL transport properties, in each of the arterial layers, which lead to dysfunctional arterial wall and stenosis that result atherosclerotic cardiovascular disease. Applying the model and the results developed in this study, one can more easily understand the initiation and development of atherosclerosis affected by LDL transport, and further explore the improvements on early diagnosis and treatment of atherosclerosis and other related cardiovascular diseases.

The microstructure details and characteristics of the endothelium and intima due to the formation of plaque/stenosis are incorporated into the present analysis. Pertinent scenarios for transport through a dysfunctional endothelium and fibrous cap within intima are invoked. The variable intima properties affected

by LDL molecule accumulation are analyzed, and its impact on the hydraulic and molecular transport in a thickened arterial wall is examined. Lower porosity by lipid blockage results in a lower permeability, which is diminished by thickening of effective fiber due to more space between the fibers as a result of stenosis.

### Conflict of interest statement

There is no conflict of interest in this paper.

### References

- Ai, L., Vafai, K., 2006. A coupling model for macromolecule transport in a stenosed arterial wall. *International Journal of Heat and Mass Transfer* 49, 1568–1591.
- American Heart Association, 2005. Heart Disease and Stroke Statistics—2005 update. American Heart Association, Dallas.
- American Heart Association, 2006. Heart Disease and Stroke Statistics—2006 update. American Heart Association, Dallas.
- American Heart Association, 2007. Heart Disease and Stroke Statistics—2007 update. American Heart Association, Dallas.
- American Heart Association, 2008. Heart Disease and Stroke Statistics—2008 update. American Heart Association, Dallas.
- Buchanan Jr., J.R., Kleinstreuer, C., 1997. Computational analysis of particle-hemodynamics in a stenosed artery segment. *American Society of Mechanical Engineers, Fluids Engineering Division (Publication) FED, Bio-Medical Fluids Engineering* 21, 8.
- Buckwalter, J.A., Rosenberg, L.C., 1982. Electron microscopic studies of cartilage proteoglycans. *The Journal of Biological Chemistry* 257 (16), 9830–9839.
- Chung, S., Vafai, K., 2012. Effect of the fluid-structure interactions on low-density lipoprotein within a multi-layered arterial wall. *Journal of Biomechanics* 45, 371–381.
- Curry, F.E., 1984a. Mechanics and thermodynamics of transcapillary exchange. *Handbook of Physiology, Section 2, The Cardiovascular System*, 4. American Physiological Society, Bethesda, MD, pp. 309–374.
- Curry, F.E., 1984b. Determinants of capillary permeability: a review of mechanism based on capillary studies in the frog. *Circulation Research* 59 (4), 367–380.
- Curry, F.E., Michel, C.C., 1980. A fiber matrix model of capillary permeability. *Microvascular Research* 20, 96–99.
- Dabagh, M., Jalali, P., Tarbell, J.M., 2009. The transport of LDL across the deformable arterial wall: the effect of endothelial cell turnover and intimal deformation under hypertension. *American Journal of Physiology—Heart Circulatory Physiology* 297, 983–996.
- Frank, J.S., Fogelman, A.M., 1989. Ultrastructure of the intima in WHHL and cholesterol-fed rabbit aorta prepared by ultra-rapid freezing and freeze-etching. *Journal of Lipid Research* 30, 967–978.
- Fry, D.L., 1985. Mathematical models of arterial transmural transport. *The American Journal of Physiology* 248, H240–H263.
- Gillum, R.F., 1995. Epidemiology of aortic aneurysm in the United States. *Journal of Clinical Epidemiology* 48, 1289–1298.
- Happel, J., Brenner, H., 1965. *Low Reynolds number hydrodynamics: with special applications to particulate media*. Prentice-Hall, Englewood Cliffs N. J.
- Hossain, S.S., Hossainy, S.F.A., Bazilevs, Y., Calo, V.M., Hughes, T.J.R., 2011. Mathematical modeling of coupled drug and drug-encapsulated nanoparticle transport in patient-specific coronary artery walls. *Computational Mechanics* 49 (2), 213–242.
- Huang, Y., Weinbaum, S., Rumschitzki, D., Chien, S., 1992. Fiber matrix model for the growth of macromolecular leakage spots in the arterial intima. *Advanced in Biological Heat and Mass Transfer* 231, 81–92.
- Huang, Y., Rumschitzki, D., Chien, S., Weinbaum, S., 1994. A fiber matrix model for the growth of macromolecular leakage spots in the arterial intima. *Journal of Biomechanical Engineering* 116, 430–445.
- Hunag, Y., Rumschitzki, D., Chien, S., Weinbaum, S., 1997. Fiber matrix model for the filtration through fenestral pores in a compressible arterial intima. *The American Journal of Physiology* 272, 2023–2039.
- Huang, Z.J., Tarbell, J.M., 1997. Numerical simulation of mass transfer in porous media of blood vessel walls. *The American Journal of Physiology* 273, H464–H477.
- Karner, G., Perktold, K., Zehentner, H.P., 2001. Computational modeling of macromolecule transport in the arterial wall. *Computer Methods in Biomechanics and Biomedical Engineering* 4, 491–504.
- Katz, M.A., 1985. New formulation of water and macromolecular flux which corrects for non-ideality: theory and derivation, predictions, and experimental results. *Journal of Theoretical Biology* 112, 369–401.
- Kedem, O., Katchalsky, A., 1958. Thermodynamic analysis of the permeability of biological membranes to non-electrolytes. *Biochimica et Biophysica Acta* 27, 229–246.
- Khakpour, M., Vafai, K., 2008. Effects of gender-related geometrical characteristics of aorta—iliac bifurcation on hemodynamics and macromolecule concentration distribution. *International Journal of Heat and Mass Transfer* 51, 5542–5551.
- Khanafer, K., Berguer, R., 2009. Fluid—structure interaction analysis of turbulent pulsatile flow within a layered aortic wall as related to aortic dissection. *Journal of Biomechanics* 42, 2642–2648.
- Khanafer, K., Bull, J.L., Berguer, R., 2009. Fluid—structure interaction of turbulent pulsatile flow within a flexible wall axisymmetric aortic aneurysm model. *European Journal of Mechanics B-Fluids* 28, 88–102.
- Lark, M.W., Yeo, T., Mar, H., Lara, S., Hellstrom, I., Hellstrom, K., Wight, T.N., 1988. Arterial chondroitin sulfate proteoglycan: localization with a monoclonal antibody. *The Journal of Histochemistry and Cytochemistry* 36, 1211–1221.
- Liu, X., Fan, Y., Deng, X., 2011. Effect of the endothelial glycocalyx layer on arterial LDL transport under normal and high pressure. *Journal of Theoretical Biology* 283 (1, 21), 71–81.
- Meyer, G., Merval, R., Tedgui, A., 1996. Effects of pressure-induced stretch and convection on low-density lipoprotein and albumin uptake in the rabbit aortic wall. *Circulation Research* 79 (3), 532–540.
- Michel, C.C., Curry, F.E., 1999. Microvascular permeability. *Physiological Reviews* 79, 703–761.
- Prosi, M., Zunino, P., Perktold, K., Quarteroni, A., 2005. Mathematical and numerical models for transfer of low-density lipoproteins through the arterial walls: a new methodology for the model set up with applications to the study of disturbed luminal flow. *Journal of Biomechanics* 38, 903–917.
- Tarbell, J.M., 2003. Mass transport in arteries and the localization atherosclerosis. *Annual Review of Biomedical Engineering* 5, 79–118.
- Tada, S., Tarbell, J.M., 2004. Internal elastic lamina affects the distribution of macromolecules in the arterial wall: a computational study. *American Journal of Physiology* 287, H905–H913.
- Wang, D.S., Dake, M.D., 2006. In: Rousseau, H., Verhoye, J.P., Heautot, J.F. (Eds.), *Endovascular Therapy for Aortic Dissection*. Thoracic Aortic Diseases Springer, New York, NY.
- Weinbaum, S., Tsay, R., Curry, F.E., 1992. A three-dimensional junction-pore-matrix model for capillary permeability. *Microvascular Research* 44, 85–111.
- Wen, G.B., Weinbaum, S., Ganatos, P., Pfeffer, R., Chien, S., 1988. On the time dependent diffusion of macromolecules through transient open junctions and their subendothelial spread. 2. Long time model for interaction. *Journal of Theoretical Biology* 135, 219–253.
- Yang, N., Vafai, K., 2006. Modeling of low-density lipoprotein (LDL) transport in the artery—effects of hypertension. *International Journal of Heat and Mass Transfer* 49, 850–867.
- Yang, N., Vafai, K., 2008. Low-density lipoprotein (LDL) transport in an artery—a simplified analytical solution. *J. Int. Heat Mass Transfer* 51, 497–505.
- Yuan, F., Chien, S., Weinbaum, S., 1991. A new view of convective-diffusive transport processes in the arterial intima. *Journal of Biomechanical Engineering* 113, 314–329.